(North-Holland, Amsterdam, 1980).
[12]A. Klein, in *Dynamical Structure of Nuclear States*, edited by D. J. Rowe *et al.* (Univ. of Toronto Press, Toronto, 1972).
[13]R. M. Dreizler and A. Klein, Phys. Rev. C 7, 512 (1973).
[14]S. Okubo, J. Math. Phys. (N.Y.) 16, 528 (1975).
[15]This representation also appears in the work of D. Janssen, R. V. Jolos, and F. Donau, Nucl. Phys. A224, 93 (1974). The reasoning used in this paper can be justified, however, only if the operators which correspond to our b_μ represent quasibosons. For this reason, the physical significance of the quantum number N cannot be assigned unambiguously.
[16]T. Holstein and H. Primakoff, Phys. Rev. 58, 1098 (1940).
[17]A. Arima and F. Iachello, Ann. Phys. (N.Y.) 99, 253 (1976).
[18]A. Arima and F. Iachello, Phys. Rev. Lett. 40, 40 (1978).
[19]A. Arima and F. Iachello, Ann. Phys. (N.Y.) 111, 201 (1978).
[20]Because the Lie algebra maps onto a subspace of the full boson space, the x and p operators are not strictly canonical.
[21]We have omitted the zero-point energy, which first contributes to $\mathfrak{U}^{(1)}$.
[22]G. Gneuss and W. Greiner, Nucl. Phys. A171, 449 (1971).
[23]J. M. Eisenberg and W. Greiner, *Nuclear Theory*, (North-Holland, Amsterdam, 1970), Vol. I, Chap. 4.
[24]J. N. Ginocchio and M. W. Kirson, Los Alamos Scientific Laboratory Report No. LA-UR-80-1707, 1980 (to be published).

Quadrupole Effects in ^{7}Li and ^{9}Be Scattering and the Folding Model

V. Hnizdo,[a] K. W. Kemper, and J. Szymakowski
Department of Physics, Florida State University, Tallahassee, Florida 32306
(Received 5 January 1981)

The inclusion of the quadrupole moment of ^{7}Li and ^{9}Be in coupled-channels calculations removes the need to renormalize the real double-folded potential, obtained from an effective nucleon-nucleon interaction, for $^7\text{Li}+^{54}\text{Fe}$, ^{40}Ca and $^9\text{Be}+^{40}\text{Ca}$ elastic scattering.

PACS numbers: 21.40.Dp, 25.70.Hi, 21.30.+y

In the double-folding model, the optical potential is obtained by folding an effective nucleon-nucleon interaction with the projectile- and target-density distributions. Elastic scattering of the lighter heavy ions has been in general successfully described[1-3] by using the effective nucleon-nucleon interaction M3Y,[4] which is based on a realistic G matrix, to generate a double-folded real part of the optical potential. However, the scattering of ^{6}Li (Refs. 5 and 6) and ^{9}Be (Ref. 7) projectiles appears to be anomalous in the sense that the M3Y interaction has to be reduced by a factor of about 2 to reproduce the data. Recently, the need for a renormalization of the double-folded potential by a factor of $\sim\frac{1}{2}$ has been shown for ^{7}Li scattering.[8,9] Satchler[7] has suggested that the anomalous behavior of ^{6}Li and ^{9}Be could be connected with the very small breakup energies of these two nuclei: only 1.47 MeV and 1.57 MeV for $^6\text{Li}\rightarrow\alpha+d$ and $^9\text{Be}\rightarrow 2\alpha+n$, respectively. The nuclei ^{7}Li and ^{9}Be have, however, another important property, large static quadrupole moments: $-4.5\pm0.5\ e\cdot\text{fm}^2$ for ^{7}Li (Ref. 10) and $+4.9\pm0.3\ e\cdot\text{fm}^2$ for ^{9}Be (Ref. 11). Blair[12] first suggested that ground-state quadrupole moments could be important in elastic scattering of heavy ions. Recent work[13] has demonstrated that there are significant quadrupole contributions to ^{10}B elastic scattering. In this Letter we show that when the strong quadrupole effects in the scattering of ^{7}Li and ^{9}Be projectiles are treated explicitly in coupled-channels calculations, no renormalization of the real double-folded potential is needed to reproduce the data in the cases investigated.

The targets ^{40}Ca and ^{54}Fe were chosen for the present study to minimize the role of strongly coupled target excited states, which could obscure the effects due to the projectile quadrupole moment. We analyzed previously measured data for $^7\text{Li}+^{54}\text{Fe}$ elastic scattering and inelastic scattering to the first excited state in ^{7}Li taken at $E_{\text{lab}}=48$ MeV (Ref. 14), and for $^7\text{Li}+^{40}\text{Ca}$ elastic scattering at 34 MeV (Ref. 15), and our new data for $^9\text{Be}+^{40}\text{Ca}$ elastic scattering at 40 MeV. The $^9\text{Be}+^{40}\text{Ca}$ data were taken at the Florida State University tandem laboratory and details of these types of measurements and their sources of errors are given in Ref. 3. The Be beam was produced by accelerating BeH^- ions obtained by flowing ammonia onto a Be cone in our inverted sputter source. The $^9Be + ^{40}Ca$ angular distribution extends to $\sigma/\sigma_R \simeq 10^{-5}$ ($\theta_{c.m.} \simeq 120°$), and has an absolute uncertainty of $\pm 6\%$.

The data for $^7Li + ^{54}Fe$ elastic scattering at 48 MeV were analyzed in terms of the double-folding model in Ref. 8, where a renormalization factor $N = 0.51$ was found for the real double-folded potential. We studied the effects of the quadrupole moment of $^7Li + ^{54}Fe$ scattering by including a quadrupole term in the optical potential, and performed coupled-channels calculations[16] with the renormalization factor of the real folded potential fixed at $N = 1.0$. The real monopole part of the potential was obtained by folding the M3Y interaction with spherical projectile and target nucleon densities obtained from electron-scattering work, while the imaginary monopole part had the phenomenological Woods-Saxon form. The details of the procedure are given in Ref. 8. The real part of the quadrupole term was calculated by folding the M3Y interaction with the quadrupole density of the projectile and the spherical density of the target. For simplicity, the radial quadrupole density was assumed to have a derivative form

$$\rho_2^{ij}(r) = \delta_2^{ij} d\rho_0(r)/dr, \tag{1}$$

where $\rho_0(r)$ is the spherical density of the projectile, and δ_2^{ij} is the quadrupole deformation length for the coupling of the ith state with the jth state in the projectile. The deformation length δ_2^{00} for the reorientation (self-coupling) of the projectile ground state was fixed by normalizing the quadrupole density $\rho_2^{00}(r)$ to the intrinsic electric quadrupole moment Q_{20} of the projectile:

$$(16\pi/5)^{1/2}\int \rho_2^{00}(r) r^4 dr = (A/Ze) Q_{20}. \tag{2}$$

In view of the absence of a model-independent knowledge of the deformation of the neutron distribution, this seemed to be the simplest assumption. There is some evidence[17] that this assumption is correct for ^7Li. The rotational model was assumed, with the ground $\frac{3}{2}^-$ state and the $\frac{1}{2}^-$ (0.48-MeV) state in ^7Li belonging to the $K = \frac{1}{2}^-$ rotational band. The ground state intrinsic moment Q_{20} of ^7Li is thus given as $Q_{20} = -5Q_2 = +22.5\ e \cdot fm^2$ with the experimental value[10] of the static moment Q_2. The deformation length δ_2^{01} for the coupling between the ground and the first excited states in ^7Li was adjusted to the magnitude of the cross section[14] for the $^7Li^*(\frac{1}{2}^-$, 0.48 MeV) excitation. The resulting value $\delta_2^{01} = 2.8$ fm is in excellent agreement with the charge deformation length of 2.8 fm deduced from the experimental $B(E2, \frac{3}{2} \rightarrow \frac{1}{2})$ value[10] of $6.7\ e^2 \cdot fm^4$. The imaginary part of the quadrupole term was of the conventional, Woods-Saxon derivative form with the same deformation length as the real part.

Figure 1 shows the results of our calculations for the $^7Li + ^{54}Fe$ scattering and compares predictions based on different coupling schemes. The $N = 1.0$ prediction without quadrupole effects is seen to oscillate too strongly and completely out of phase with the experimental data. The effect of the reorientation coupling of the ground state of ^7Li is quite dramatic, as the oscillations are now damped and have the right phase. The inclusion of the $\frac{3}{2}^- - \frac{1}{2}^-$ coupling further improves the agreement with the data, resulting in a very good fit which is equivalent in the region covered by the experimental data ($\theta_{c.m.} \lesssim 55°$) to the $N = 0.51$ fit without quadrupole effects of Ref. 8. The $\frac{3}{2}^-$-$\frac{1}{2}^-$ coupling results in a prediction for the $^7Li^*(\frac{1}{2}^-$, 0.48 MeV) cross section, shown also in Fig. 1, which agrees much better in phase with the data than the distorted-wave fit of Ref. 14. The parameters of the calculations are summarized in Table I. It should be noted that the Woods-Saxon

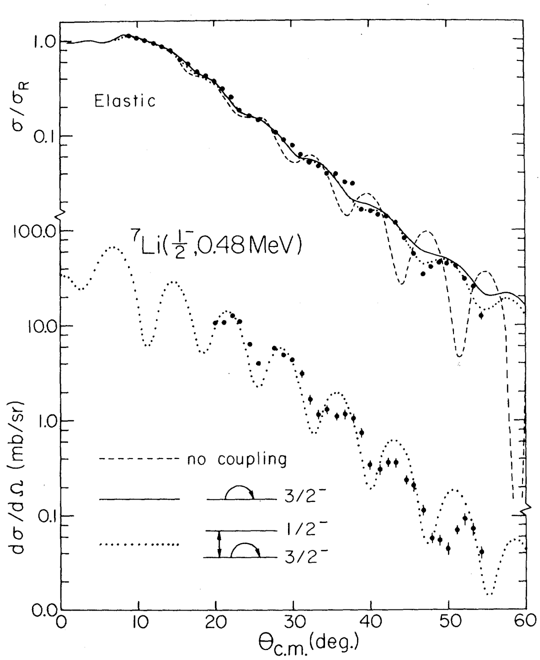

FIG. 1. Calculations based on different coupling schemes for $^7Li + ^{54}Fe$ elastic and inelastic scattering at 48 MeV. The calculations were done with N fixed at 1.0 with use of the parameters of Table I.

TABLE I. Optical-potential parameters and quadrupole deformation lengths. The potential has a double-folded real part, renormalized by the factor N, and a Woods-Saxon imaginary part.

System	N	W (MeV)	r_I [a] (fm)	a_I (fm)	δ_2^{00} (fm)	δ_2^{01} (fm)
$^7Li + ^{54}Fe$	1.0	31.6	1.00	0.97	3.4	2.8
$^7Li + ^{40}Ca$	0.60	20.0	1.00	1.00	0	0
	1.0	27.0	1.00	1.00	3.4	2.8
$^9Be + ^{40}Ca$	0.66	22.9	1.22	0.71	0	0
	1.0	35.0	1.22	0.71	2.5	0
	1.0	40.0	1.22	0.71	2.5	2.5

[a] $R_I = r_I (A_p^{1/3} + A_t^{1/3})$; charge radius $R_c = 1.3\, A_t^{1/3}$ fm.

imaginary potential was the same as that of Ref. 8. Using the same procedure, we were also able to reproduce the main features of the data[15] for $^7Li + ^{40}Ca$ elastic scattering at 34 MeV with the renormalization factor fixed at $N = 1.0$. For these data, a renormalization $N = 0.60$ was found in Ref. 8, where the fit still had much too deep minima at the backward angles. The results of the $^7Li + ^{40}Ca$ calculations are shown in Fig. 2 and the calculation parameters are given in Table I.

We analyzed our $^9Be + ^{40}Ca$ elastic-scattering data taken at 40 MeV using a procedure similar to the one used for the ^7Li scattering. The spherical density of ^9Be had a proton part determined from electron scattering,[18] with a neutron part adjusted so that the difference between the neutron and proton rms radii, after a deconvolution of the proton size, was 0.38 fm (method B of Ref. 7). In agreement with Satchler,[7] we found that fitting the data without an explicit treatment of the quadrupole effects required a substantial reduction of the real double-folded potential, resulting in a renormalization factor of $N = 0.66$. This renormalization is not, however, as drastic as the factor of $N \sim 0.3$ reported recently[19] for $^9Be + ^{40}Ca$ elastic scattering at $E_{lab} = 45$ and 60 MeV. In the coupled-channels calculations, we set $N = 1.0$ and assumed the $K = \frac{3}{2}^-$ rotational band for ^9Be. The value of δ_2^{00} for the reorientation coupling of the $\frac{3}{2}^-$ ground state of ^9Be was determined from the experimental value[11] $Q_2 = 5\ e \cdot fm^2$ of the static quadrupole moment of ^9Be. Since it is not possible to observe the ^9Be projectile excitation in the detection setup we used, the effect of the coupling between the ground state and the $\frac{5}{2}^-$ (2.43-MeV) state in ^9Be was difficult to assess. We thus simply set $\delta_2^{01} = \delta_2^{00}$ for this coupling. The strength W of the imaginary Woods-Saxon potential was allowed to adjust for the coupling effects. The results of the calculations are compared with the data in Fig. 2. It can be seen that the reorientation coupling of the ^9Be ground state results in a fit which is at least as good as the fit with $N = 0.66$ and no quadrupole effects, especially at the backward angles. The $\frac{3}{2}^- - \frac{5}{2}^-$ coupling with $\delta_2^{01} = \delta_2^{00}$ was perhaps too strong, as it was not possible to adjust fully for the inclusion of this effect by a change in W only. Adjustments in the geometry of the imaginary potential can be done reliably only when ^9Be projectile excitation data are obtained. The calculation parameters are given in Table I.

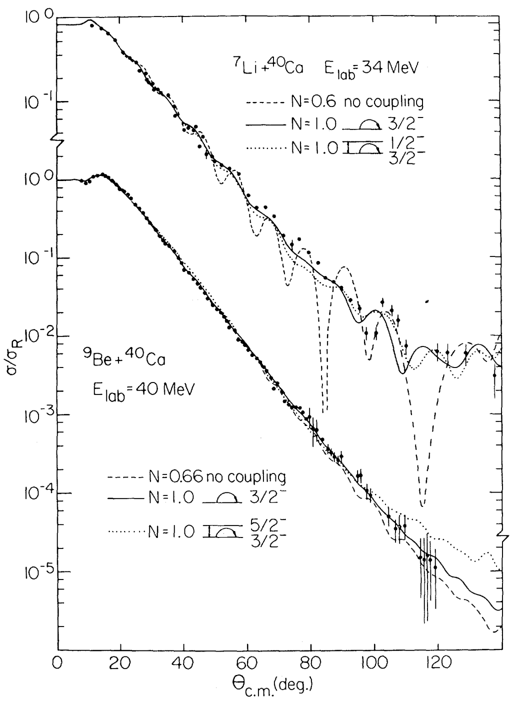

FIG. 2. Angular distributions for $^7Li + ^{40}Ca$ elastic scattering at 34 MeV and $^9Be + ^{40}Ca$ elastic scattering at 40 MeV, compared with calculations based on different coupling schemes with use of the parameters of Table I. The fits without coupling (dashed line) were obtained by allowing N to vary.

In conclusion, quadrupole effects are very important in the scattering of ^7Li and ^9Be projectiles. When these effects were treated explicitly in the coupled-channels formalism, it was not necessary to renormalize the real double-folded potential to fit the data in the cases we considered. These results give support to the double-folding model with the M3Y interaction as providing a correct first-order real part of the heavy-ion optical potential in the exterior region. Coupled-channels calculations which involve an explicit treatment of both the projectile and the target higher-order effects still impose an excessive demand on the computing time, especially at higher energies where a large number of partial waves is needed. For this reason it was not possible to carry out such calculations for the recently measured ^{9}Be $+^{28}$Si elastic-scattering data at 121 and 201.6 MeV (Ref. 20). The ^{6}Li anomaly still presents a problem since ^{6}Li has a very small quadrupole moment. However, proton and α scattering by ^{6}Li shows its 3^+ (2.18-MeV) state to be strongly excited, and it is possible that simple coupled-channels effects due to this state play an important role in ^{6}Li scattering.

This work was supported in part by the National Science Foundation. One of the authors (V.H.) gratefully acknowledges the support of the Florida State University and the Council for Scientific and Industrial Research, Pretoria.

[a]On leave from Department of Physics, University of the Witwatersrand, Johannesburg, South Africa.

[1]G. R. Satchler and W. G. Love, Phys. Rep. 55, 185 (1979).
[2]G. R. Satchler, Nucl. Phys. A329, 233 (1979).
[3]C. W. Glover *et al.*, Nucl. Phys. A337, 520 (1980).
[4]G. Bertsch *et al.*, Nucl. Phys. A284, 399 (1977).
[5]G. R. Satchler and W. G. Love, Phys. Lett. 76B, 23 (1978); G. R. Satchler, Phys. Rev. C 22, 919 (1980).
[6]D. P. Stanley, F. Petrovich, and P. Schwandt, Phys. Rev. C 22, 1357 (1980).
[7]G. R. Satchler, Phys. Lett. 83B, 284 (1979).
[8]C. W. Glover, R. I. Cutler, and K. W. Kemper, Nucl. Phys. A341, 137 (1980).
[9]J. Cook, N. M. Clarke, and R. J. Griffiths, to be published.
[10]G. J. C. van Niftrik *et al.*, Nucl. Phys. A174, 173 (1971).
[11]A. G. Blachman and A. Lurio, Phys. Rev. 153, 164 (1967).
[12]J. S. Blair, Phys. Rev. 115, 928 (1959).
[13]L. A. Parks *et al.*, Phys. Lett. 70B, 27 (1977); L. A. Parks *et al.*, Phys. Rev. C 21, 217 (1980).
[14]K. W. Kemper *et al.*, Nucl. Phys. A320, 413 (1979).
[15]R. I. Cutler, M. J. Nadworny, and K. W. Kemper, Phys. Rev. C 15, 1318 (1977).
[16]A modified version of the code CHUCK of P. D. Kunz (unpublished) was used.
[17]E. Steffens, in Proceedings of the Fifth International Symposium on Polarization Phenomena in Nuclear Physics, Santa Fe, New Mexico, 1980 (to be published).
[18]C. W. de Jager, H. de Vries, and C. de Vries, At. Data Nucl. Data Tables 14, 479 (1974).
[19]J. S. Eck *et al.*, Nucl. Phys. A334, 519 (1980).
[20]M. S. Zisman *et al.*, Phys. Rev. C 21, 2398 (1980).

Role of Thermalization for Electron Distributions in Resonance Absorption

Bandel Bezzerides and Steven J. Gitomer
Los Alamos National Laboratory, University of California, Los Alamos, New Mexico 87545
(Received 7 November 1980)

The interplay between the bulk properties of the plasma and the nonlinear particle heating due to resonance absorption is analyzed. It is shown that the dependence of the heating on the initial energy with which particles enter the heating region provides a key to understanding the formation of the time-averaged distribution.

PACS numbers: 52.50.Jm, 52.65.+z

In the last few years particle simulations have concentrated on resonance absorption as an explanation of the hot electrons observed in high-intensity laser experiments. In these simulations the heating region is continuously replenished with particles drawn from the background thermal distribution fixed at the overdense boundary.[1] This effect of the background temperature goes beyond the direct effect the temperature may have on the accelerating waves, themselves causing thermal dispersion. On the other hand, the cold-plasma limit has been used to provide some insight into the heating.[2] Limited to single-stream flow, the model cannot be used to investigate the effect of the initial energy of particles, and, more generally, the effect of thermalization, and therefore the description of the heating is transient, not permitting detailed comparison with quasi-steady simulations.

Since the heating is predominantly in the direction of the density gradient, we employ here the well-known one-dimensional (1D) capacitor mod-